# Accessory cusp expression at the enamel-dentine junction of hominin mandibular molars

Thomas W. Davies[1], Zeresenay Alemseged[2], Agness Gidna[3], Jean-Jacques Hublin[1,4], William H. Kimbel[5], Ottmar Kullmer[6,7], Fred Spoor[1,8,9], Clément Zanolli[10] and Matthew M. Skinner[1,11,12]

[1] Department of Human Evolution, Max Planck Institute for Evolutionary Anthropology, Leipzig, Germany
[2] Department of Organismal Biology and Anatomy, University of Chicago, Chicago, Illinois, United States
[3] Paleontology Unit, National Museum of Tanzania, Dar es Salaam, Tanzania
[4] Collège de France, Paris, France
[5] Institute of Human Origins, and School of Human Evolution and Social Change, Arizona State University, Tempe, Arizona, United States
[6] Department of Paleobiology and Environment, Institute of Ecology, Evolution, and Diversity, Goethe University, Frankfurt, Germany
[7] Department of Palaeoanthropology, Senckenberg Research Institute and Natural History Museum Frankfurt, Frankfurt am Main, Germany
[8] Centre for Human Evolution Research, Department of Earth Sciences, Natural History Museum, London, United Kingdom
[9] Department of Anthropology, University College London, London, United Kingdom
[10] Univ. Bordeaux, CNRS, MCC, PACEA, UMR 5199, F-33600 Pessac, France
[11] School of Anthropology and Conservation, University of Kent, Canterbury, United Kingdom
[12] Centre for the Exploration of the Deep Human Journey, University of the Witwatersrand, Johannesburg, South Africa

Corresponding author
Thomas W. Davies,
thomas_davies@eva.mpg.de

## ABSTRACT

Studies of hominin dental morphology frequently consider accessory cusps on the lower molars, in particular those on the distal margin of the tooth (C6 or distal accessory cusp) and the lingual margin of the tooth (C7 or lingual accessory cusp). They are often utilized in studies of hominin systematics, where their presence or absence is assessed at the outer enamel surface (OES). However, studies of the enamel-dentine junction (EDJ) suggest these traits may be more variable in development, morphology and position than previously thought. Building on these studies, we outline a scoring procedure for the EDJ expression of these accessory cusps that considers the relationship between these accessory cusps and the surrounding primary cusps. We apply this scoring system to a sample of Plio-Pleistocene hominin mandibular molars of *Paranthropus robustus, Paranthropus boisei, Australopithecus afarensis, Australopithecus africanus, Homo* sp., *Homo habilis* and *Homo erectus* from Africa and Asia ($n$ = 132). We find that there are taxon-specific patterns in accessory cusp expression at the EDJ that are consistent with previous findings at the OES. For example, *P. robustus* $M_1$s and $M_2$s very often have a distal accessory cusp but no lingual accessory cusp, while *H. habilis* $M_1$s and $M_2$s show the opposite pattern. The EDJ also reveals a number of complicating factors; some apparent accessory cusps at the enamel surface are represented at the EDJ only by shouldering on the ridges associated with the main

cusps, while other accessory cusps appear to have little or no EDJ expression at all. We also discuss the presence of double and triple accessory cusps, including the presence of a double lingual accessory cusp on the distal ridge of the metaconid in the type specimen of *H. habilis* (OH 7–$M_1$) that is not clear at the OES due to occlusal wear. Overall, our observations, as well as our understanding of the developmental underpinnings of cusp patterning, suggest that we should be cautious in our comparisons of accessory cusps for taxonomic interpretations.

# INTRODUCTION

Although hominin mandibular molars typically have five main cusps, extra (accessory) cusps are variably present and are common in some taxa. They are frequently present on the distal marginal ridge (between the entoconid and hypoconulid) where they are termed a tuberculum sextum (C6 or distal accessory cusp), or on the lingual marginal ridge (between the metaconid and entoconid), where they are termed a tuberculum intermedium (C7 or lingual accessory cusp—Fig. 1). Descriptions of fossil hominin teeth routinely report the presence of these accessory cusps (*Grine & Franzen, 1994*; *Johanson, White & Coppens, 1982*; *Moggi-Cecchi, Grine & Tobias, 2006*; *Moggi-Cecchi et al., 2010*; *Robinson, 1956*; *Tobias, 1991*; *Weidenreich, 1937*; *Wood, 1991*) and studies of hominin taxonomy frequently use both lingual and distal accessory cusps (*Irish et al., 2018*; *Suwa, 1990*; *Suwa, White & Howell, 1996*; *Wood & Abbott, 1983*). For example, *Wood & Abbott (1983)* stated that *Paranthropus* $M_1$s very often have a distal accessory cusp, while the $M_2$s invariably show no lingual accessory cusp. Similarly, *Suwa, White & Howell (1996)* suggested that for $M_1$ and $M_2$, the presence of a lingual accessory cusp and lack of a distal accessory cusp implied an assignment to a non-robust taxon.

For the most part, accessory cusps are recorded at the outer enamel surface (OES). While this is accurate in some cases, OES morphology can be obscured by the effects of dental occlusal wear, which can impede accurate assessment of crown morphology. For example, *Burnett, Irish & Fong (2013)* found that increasing degrees of occlusal wear in a sample of $M_2$s led to two independent observers recording fewer cusps in the teeth. Fossil hominin tooth samples are often very small, meaning that it is rarely practical to include only unworn or lightly worn teeth. Using X-ray, synchrotron and neutron microtomography, however, it is possible to image, in three dimensions, the internal dental structures of many fossil specimens (*Davies et al., 2020*; *Le Cabec, Dean & Begun, 2017*; *Martinón-Torres et al., 2019*; *Skinner et al., 2016*; *Skinner et al., 2008*; *Xing, Martinón-Torres & De Castro, 2018*; *Zanolli et al., 2020*). Accessory cusps are 'primary-definitive' traits (sensu *Nager, 1960*), a term that refers to dental features that are present at the unworn OES, but derive from the enamel-dentine junction (EDJ). By imaging the EDJ we can assess accessory cusp presence in worn teeth. In unworn and moderately worn
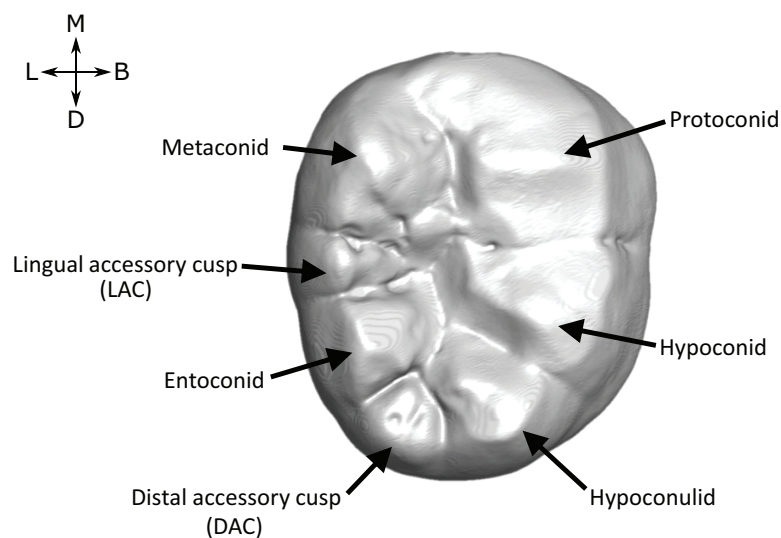
**Figure 1 Lower molar cusp layout.** An example molar (OH 7 LM$_2$, image reversed) illustrating the main cusps and the two accessory cusps examined in this study.

specimens, we can compare the OES and EDJ morphology, allowing a more detailed assessment of accessory cusp form.

Another advantage of utilizing the EDJ is that many hominin taxa have relatively thick enamel, which can make the detailed morphology of crown features difficult to assess. At the EDJ, such features often appear more distinctive, and we can assess not just the presence of accessory cusps, but their spatial relationship and position relative to other crown features. This is particularly important as a number of authors distinguish between different 'types' of lingual and distal accessory cusps. For example, there is a distinction between a 'C7' and a 'postmetaconulid' that is determined by the extent to which a lingual accessory cusp is separated from the metaconid at the OES (*Grine, 1984*). This distinction is frequently recognized in descriptions and analyses of hominin dental remains (*Grine et al., 2019*; *Kaifu, Aziz & Baba, 2005*; *Moggi-Cecchi, Grine & Tobias, 2006*; *Skinner et al., 2020*; *Suwa, Wood & White, 1994*). *Skinner et al. (2008)* also distinguished between different types of lingual and distal accessory cusps at the EDJ according to the placement of the cusp and its association with adjacent cusps, as well as identifying a number of 'doubled' accessory cusps. Further, *Ortiz et al. (2017)* found that accessory cusps visible at the OES of hominoid upper and lower molars corresponded to a wide variety of EDJ morphologies. They found a number of examples in which cusps at the OES originated from shouldering features at the EDJ, rather than distinct dentine horns, and in some cases found cusps that appear to originate entirely through enamel deposition.

Furthermore, advances in our understanding of tooth development suggest that accessory cusps are not individually patterned, and may instead form depending on a number of upstream factors such as the size and spacing of the main cusps. For example, *Skinner & Gunz (2010)* demonstrated that accessory cusp variation on the distal margin of

**Table 1 Study sample summary.** The taxon groupings, sites and sample sizes are listed for the study sample. More information on the study sample can be found in Table S1.

| Taxon | Site | $n$ ($M_1$, $M_2$, $M_3$) |
|---|---|---|
| *P. robustus* | Drimolen and Swartkrans, South Africa | 8, 7, 5 |
| *P. boisei* | Koobi Fora and Ileret, Kenya | 2, 2, 2 |
| *A. afarensis* | Hadar, Ethiopia | 7, 10, 4 |
| *A. africanus* | Sterkfontein, South Africa | 6, 8, 8 |
| Hominidae gen. et sp. indet. | Koobi Fora, Kenya | 1, 1, 0 |
| *Homo* sp. | Drimolen, Sterkfontein and Swartkrans, South Africa; Koobi Fora, Kenya; Shungura Formation, Ethiopia | 7, 6, 4 |
| *H. habilis* | Koobi Fora, Kenya; Olduvai Gorge, Tanzania; Shungura Formation, Ethiopia | 5, 3, 5 |
| *H. erectus* (Africa) | Baringo and Koobi Fora, Kenya; Olduvai Gorge, Tanzania | 4, 6, 4 |
| *H. erectus* (Asia) | Sangiran, Indonesia; Chinese Apothecary | 3, 8, 1 |
| MP *Homo* | Tighenif, Algeria | 1, 2, 2 |

Note:
MP, Middle Pleistocene.

the EDJ of *Pan* mandibular molars was consistent with predictions of a patterning cascade model (*Jernvall, 2000*; *Jernvall & Thesleff, 2000*). *Hunter et al. (2010)* and *Moormann, Guatelli-Steinberg & Hunter (2013)* demonstrated the predictions of the model were consistent with variation in Carabelli's trait expression in human upper molars (the latter having been suggested to play a role to increase the functional occlusal area of the tooth; *Fiorenza et al., 2020*). Moreover, *Ortiz et al. (2018)* found similar support for variation in these and other accessory cusps in hominoids. These observations raise two important questions, in particular for the use of these accessory cusps as characters in taxonomic and phylogenetic studies. Are accessory cusps recorded at the OES in hominins always developmentally homologous? And does the patterning cascade model mean that accessory cusps are particularly liable to originate independently in separate hominin lineages?

In this paper, we use microtomography to image the EDJ and OES expression of accessory cusps on the distal and lingual margins of Plio-Pleistocene hominin lower molars. We score accessory cusp expression at the EDJ, considering variation in the placement of lingual and distal accessory cusps with respect to adjacent cusps. We discuss the use of this system, and accessory cusps generally, for taxonomic distinction, and consider the impact of several developmental complexities on the use of accessory cusps in future studies.

## METHODS

### Study sample

The study sample is summarized in Table 1 and consists of 132 molars from a range of hominin taxa spanning three genera, *Australopithecus*, *Paranthropus* and *Homo* (full study sample can be found in Table S1). The study sample was selected to cover a number of well-sampled Plio-Pleistocene hominin species to facilitate comparisons between taxa. We were not able to include some samples such as *Australopithecus anamensis* and Laetoli

*Australopithecus afarensis* as only a small number of specimens have sufficient tissue contrast to image the EDJ. Samples containing only a small number of individuals, such as *Paranthropus boisei* and molars from Tighenif, are excluded from frequency tables and figures, but are discussed separately. *Homo* specimens from Africa were grouped as *Homo habilis* or *Homo erectus* where possible, however there are a number of specimens for which a specific attribution is not available, or there is disagreement over their attribution. These specimens are grouped as *Homo* sp., with the acknowledgement that this group is very likely heterogeneous. Images and descriptions of the OES and EDJ morphology of all specimens, as well as a number of antimeres not included in the main sample, can be found in the Supplemental Index.

## Microtomography

Microtomographic scans for each molar were obtained using a SkyScan 1,172 or SkyScan 1173 at 100–130 kV and 90–130 µA, a BIR ACTIS 225/300 scanner at 130 kV and 100–120 µA, a Diondo d3 at 100–140 kV and 100–140 µA, a X8050-16 Viscom AG equipment at 115–125 kV and 350-600 µA and reconstructed as 16-bit tiff stacks with an isometric voxel resolution ranging from 13-45 microns (two teeth, OH 16 LLM2 and LLM3, are scanned at 60 microns, but only the higher resolution antimeres are included in summary statistics).

Sangiran specimens S7-42, S7-78 and SMF-8865 were scanned using neutron microtomography at the ANTARES Imaging facility (SR4a beamline) of the Forschungs-Neutronenquelle Heinz Maier-Leibnitz (Research Neutron Source; FRM II reactor) of the Technische Universität München (see *Zanolli et al., 2020*). The neutron beam originated from the cold source of the FRM II reactor, with an energy range from 3 to 20 meV, a collimation ratio of L/D = 500 (the ratio between the sample-detector distance and collimator aperture) and an intensity of $6.4 \times 10^7$ n/cm$^2$s. A 20 µm Gadox screen was used to detect neutrons. Both a cooled, charge-coupled device camera (ikon-L 936; Andor) and cooled complementary metal-oxide semiconductor camera (Neo 5.5 sCMOS; Andor) were used as detectors. The final virtual volume of these specimens was reconstructed with an isotropic voxel size of 20.45 µm.

Sangiran specimens S7-20, S7-62, S7-64 and S7-65, as well as both Chinese Apothecary specimens (CA 804 and CA 808), were scanned on beamline ID 19 at the European Synchrotron Radiation Facility (ESRF, Grenoble, France) using the protocol outlined in *Smith et al. (2018)*. These data were downloaded from the European Synchrotron Radiation Facility Paleontological Microtomographic Database (http://paleo.esrf.eu).

## Segmentation

For the majority of specimens, TIFF stacks were filtered using either a mean of least variance filter (kernel size one) or a 3D median filter, followed by a mean of least variance filter (each with a kernel size of three), implemented using MIA open source software (*Wollny et al., 2013*). Filtered image stacks were segmented in Avizo 6.3 (*Visualization Sciences Group, 2010*) using a seed growing watershed algorithm employed via a custom Avizo plugin to segment enamel from dentine, before being checked manually.
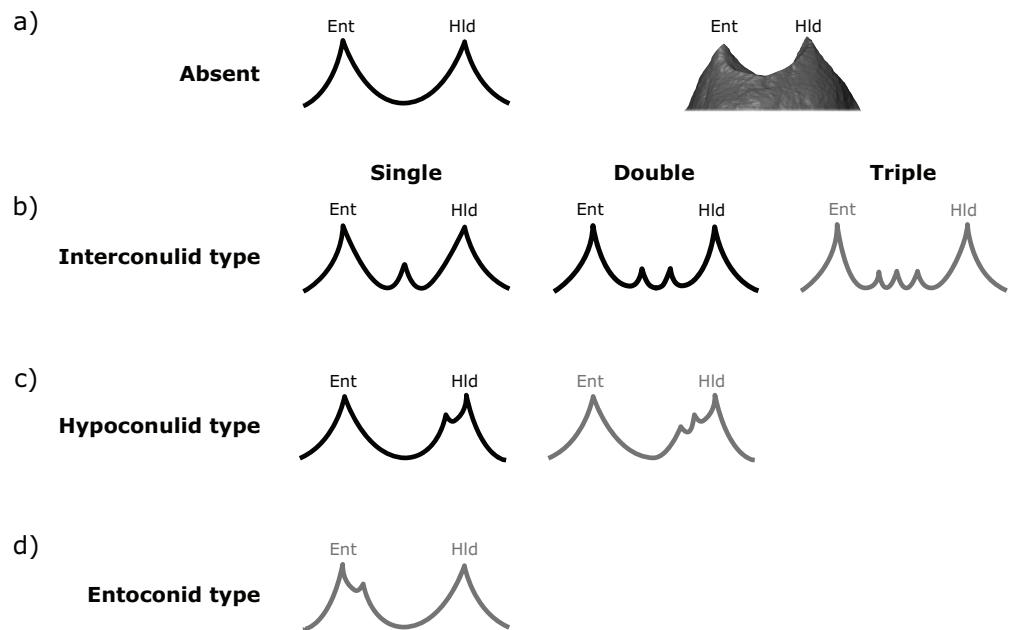
**Figure 2 Scoring system for characterizing distal accessory cusp (DAC) variation at the EDJ.** Distal accessory cusps may be scored as (A) absent, (B) interconulid type, (C) hypoconulid type, or (D) entoconid type. An example EDJ surface is also shown (a; StW 309A). Types shown in grey are rare according to our observations. Ent, Entoconid; Hld, Hypoconulid.

In specimens with particularly poor contrast between tissue types, enamel and dentine were segmented using the magic wand tool in Avizo v.8.0 (FEI Visualization Sciences Group) with manual corrections and use of the interpolation where enamel and dentine could not be precisely demarcated (For more details, see *Zanolli et al., 2019*). Once enamel and dentine were segmented, a triangle-based surface model of the EDJ was produced using the unconstrained smoothing parameter in Avizo and then saved in polygon file format (.ply).

## Scoring system

All specimens were assessed visually and scored on rotatable 3D models (2D images in occlusal, lingual and distal views at OES and EDJ are available in the SOM, along with a written assessment of accessory cusp morphology for each specimen). Each tooth in the sample was scored at the EDJ using the .ply surface model, making reference to the original CT stack when necessary. The level of tissue distinction present in the scan was also assessed as good, moderate or poor. Since accessory cusp features can be very small in some cases, these categories allow us to assess the likelihood of accessory cusps being missed at the EDJ. The scoring systems were adapted from *Skinner et al. (2008)* and expanded to include new types that are present in this sample (Figs. 2 and 3).

Importantly, given the variation in number and position of accessory cusps, as well as doubts over their developmental homology (*Skinner et al., 2008*; *Ortiz et al., 2017*), we do not think it is feasible to use the terms cusp 6 and cusp 7. Instead, we refer to distal
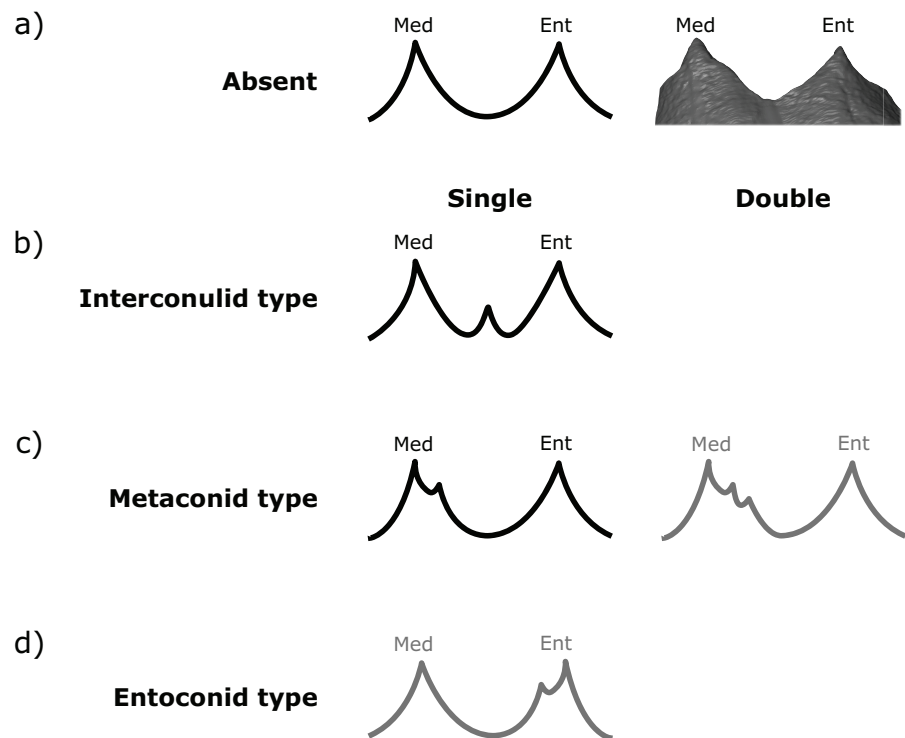
**Figure 3 Scoring system for characterizing lingual accessory cusp (LAC) variation at the EDJ.** Lingual accessory cusps may be scored as (A) absent, (B) interconulid type, (C) metaconid type, or (D) entoconid type. An example EDJ surface is also shown (a; StW 309A). Types shown in grey are rare according to our observations. Ent, Entoconid; Med, Metaconid.

accessory cusps (DAC) for those appearing on the distal crown margin between the hypoconulid and the entoconid, and to lingual accessory cusps (LAC) for those appearing on the lingual crown margin between the metaconid and entoconid. These terms will be used to describe cusps at the OES and the EDJ, but we will refer to the EDJ unless stated otherwise.

Both DACs and LACs can appear in three forms at the EDJ, reflecting their developmental origin and association (or lack thereof) with primary cusps. For DACs, these are 'hypoconulid type' for those appearing on the distal crest of the hypoconulid, 'entoconid type' for those appearing on the distal crest of the entoconid, and 'interconulid type' for those appearing on the marginal ridge between the hypoconulid and entoconid (Fig. 2). These types can appear in isolation or in combination and in single, double or triple forms. For LACs, these are 'metaconid type' for those appearing on the distal crest of the metaconid, 'entoconid type' for those appearing on the mesial crest of the entoconid and 'interconulid type' for those appearing on the marginal ridge between the metaconid and entoconid (Fig. 3). As with DACs, these LAC types can appear in isolation or in combination and in single or double forms.
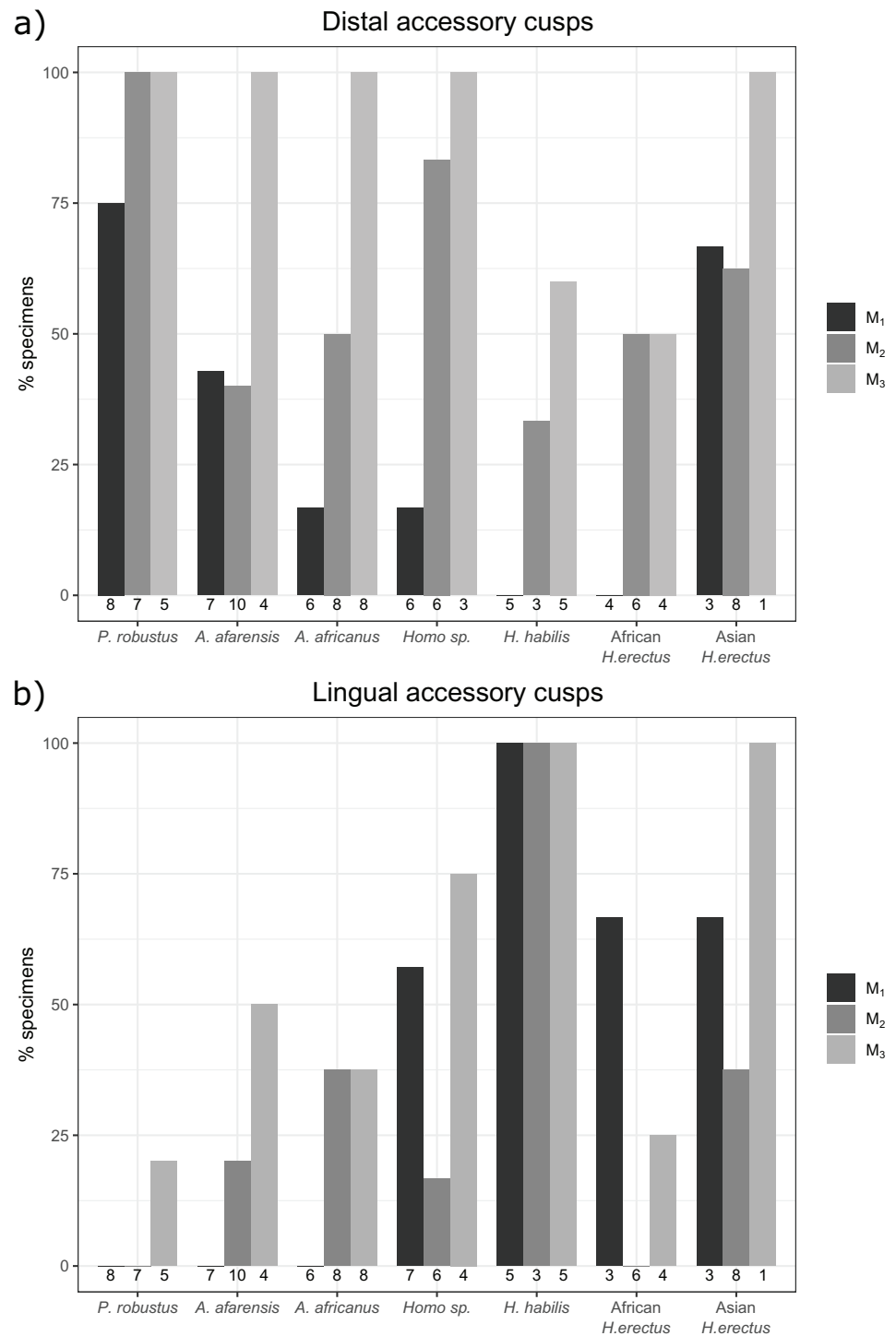
**Figure 4 Overall distal and lingual accessory cusp frequencies by tooth type and taxon.** (A) The frequency of distal accessory cusp presence, of any type, in each taxon for the $M_1$, $M_2$ and $M_3$. (B) The frequency of lingual accessory cusp presence, of any type, in each taxon for the $M_1$, $M_2$ and $M_3$. The numbers beneath each bar show the sample size.
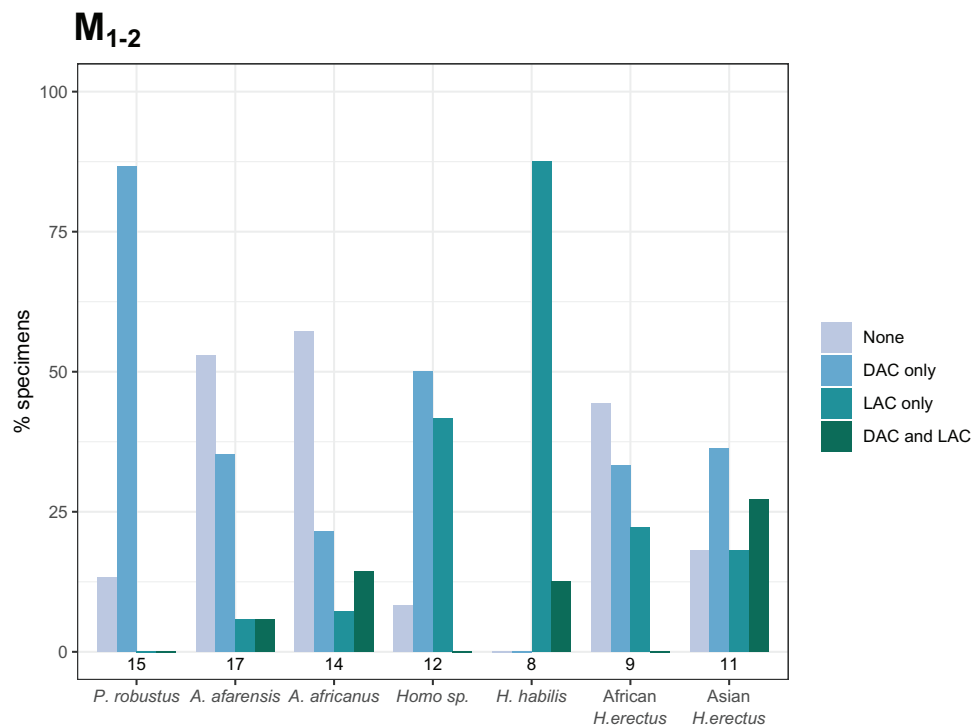
**Figure 5 Combined distal and lingual accessory cusp presence/absence frequency for M₁s and M₂s.** The frequencies shown indicate, for each taxon, the proportion of M₁s and M₂s with each combination of distal and lingual accessory cusp presence/absence. M₃s are excluded here—see text. Numbers underneath the bars indicate sample sizes for each group. Abbreviations: DAC, distal accessory cusp; LAC, Lingual accessory cusp.

## RESULTS

### Taxon specific patterns

The overall frequency of distal and lingual accessory cusps of any type is summarized in Fig. 4. The frequency of DAC presence increases along the tooth row in most taxa, with a few minor exceptions (in *A. afarensis* and Asian *H. erectus* DACs are marginally less frequent in M₂s than M₁s, but it is still highest in the M₃). This pattern is not as clear in the LACs, although six out of seven groups have the highest, or equal highest, frequency of LACs in the M₃s. DACs are particularly frequent in *P. robustus*; all M₂s and M₃s, and 6/8 (75%) of the M₁s, have at least one DAC. A similar pattern is seen in *P. boisei* – all 6 molars included have one or more DACs. There are no DACs in the M₁s of *H. habilis* or African *H. erectus*. A contrasting pattern is seen in the LACs; they are rare in *Paranthropus* (only SK 22 M₃ and KNM-ER 25520 have LACs), absent in the M₁s of *Australopithecus*, but are more common in *Homo*. All *H. habilis* teeth included here have a LAC, as well as more than 50% of the M₁s of *Homo* sp., and African and Asian *H. erectus*. *Homo* sp., as well as African and Asian *H. erectus*, appear to be differentiated from *H. habilis* by having fewer M₂ LACs than the latter. However, only three *H. habilis* M₂s were included, so this pattern should be treated with caution. When the presence/absence of both accessory cusps is considered together, there are clear patterns in the

**Table 2 Presence/absence frequencies of distal accessory cusp (DAC) types.** The presence/absence frequency of each type of DAC is shown for the $M_1$, $M_2$ and $M_3$ for each taxon. An asterisk indicates that frequencies exceed 100% due to the presence of multiple types of DAC in one or more specimens.

| Taxon | n ($M_1$, $M_2$, $M_3$) | $M_1$ (%) | | | $M_2$ (%) | | | $M_3$ (%) | | |
|---|---|---|---|---|---|---|---|---|---|---|
| | | Ent | Int | Hld | Ent | Int | Hld | Ent | Int | Hld |
| *P. robustus* | 8, 7, 5 | 0 | 62.5 | 12.5 | 0 | 85.7 | 28.6* | 0 | 100 | 20* |
| *A. afarensis* | 7, 10, 4 | 0 | 42.9 | 0 | 0 | 30 | 10 | 0 | 100 | 0 |
| *A. africanus* | 6, 8, 8 | 0 | 16.7 | 0 | 0 | 50 | 12.5 | 0 | 87.5 | 37.5* |
| *Homo sp.* | 6, 6, 3 | 0 | 16.7 | 0 | 0 | 16.7 | 66.7 | 0 | 100 | 0 |
| *H. habilis* | 5, 3, 5 | 0 | 0 | 0 | 0 | 33.3 | 0 | 20 | 40 | 40 |
| African *H. erectus* | 4, 6, 4 | 0 | 0 | 0 | 0 | 50 | 0 | 25 | 25 | 25 |
| Asian *H. erectus* | 3, 8, 1 | 0 | 33.3 | 33.3 | 0 | 37.5 | 25 | 0 | 100 | 0 |

Note:
Abbreviations: Ent, Entoconid type; Int, Interconulid type; Hld, Hypoconulid type.

**Table 3 Presence/absence frequencies of lingual accessory cusp (LAC) types.** The presence/absence frequency of each type of LAC is shown for the $M_1$, $M_2$ and $M_3$ for each taxon.

| Taxon | n ($M_1$, $M_2$, $M_3$) | $M_1$ (%) | | | $M_2$ (%) | | | $M_3$ (%) | | |
|---|---|---|---|---|---|---|---|---|---|---|
| | | Med | Int | Ent | Med | Int | Ent | Med | Int | Ent |
| *P. robustus* | 8, 7, 5 | 0 | 0 | 0 | 0 | 0 | 0 | 0 | 20 | 0 |
| *A. afarensis* | 7, 10, 4 | 0 | 0 | 0 | 10 | 10 | 0 | 0 | 50 | 0 |
| *A. africanus* | 6, 8, 8 | 0 | 0 | 0 | 37.5 | 0 | 0 | 37.5 | 12.5 | 12.5 |
| *Homo* sp. | 7, 6, 4 | 57.1 | 0 | 0 | 16.7 | 0 | 0 | 25 | 50 | 0 |
| *H. habilis* | 5, 3, 5 | 80 | 20 | 0 | 66.7 | 33.3 | 0 | 0 | 100 | 0 |
| African *H. erectus* | 3, 6, 4 | 66.7 | 33.3 | 0 | 0 | 0 | 0 | 25 | 0 | 0 |
| Asian *H. erectus* | 3, 8, 1 | 66.7 | 0 | 0 | 25 | 25 | 0 | 0 | 100 | 0 |

Note:
Abbreviations: Med, Metaconid type; Int, Interconulid type; Ent, Entoconid type.

combined $M_1$ and $M_2$ sample (Fig. 5—the $M_3$s have been excluded here as accessory cusps are more frequent and variable in form in the $M_3$s than $M_1$s and $M_2$s, but the combined DAC and LAC figures for each individual tooth position can be found in Fig. S1). *Paranthropus robustus* $M_1$s and $M_2$s most often have a DAC and no LAC (13/15). *Homo habilis* $M_1$s and $M_2$s show the opposite pattern, most often having a LAC and no DAC (7/8), with only one $M_2$ having a DAC and LAC (OH 7 $M_2$, which has a double DAC). Other groups are less consistent. *Australopithecus afarensis* $M_1$s and $M_2$s most often have no accessory cusps or only a DAC, which is similar to the pattern seen in *Australopithecus africanus*. In both of these taxa all specimens that do have a LAC are $M_2$s rather than $M_1$s.

## Accessory cusp types

Tables 2 and 3 show the presence/absence frequencies of each type of DAC (Fig. 2) and LAC (Fig. 3). Table 2 shows that interconulid type DACs are present much more often than the other types. Hypoconulid types are the next most frequent, but they are more
| | M₁ | DAC | LAC | M₂ | DAC | LAC | M₃ | DAC | LAC |
|---|---|---|---|---|---|---|---|---|---|
| | | | | DNH 60C | ○○ | | | | |
| *P. robustus* | DNH 60B | ○ | | | | | | | |
| | | | | | | | DNH 75 | ○○ | |
| | | | | SK 1 | ○ | | | | |
| | | | | SK 5 | ◉ | | | | |
| | SK 6 | ○ | | SK 6 | ○ | | SK 6 | ○◉ | |
| | | | | | | | SK 22 | ○ | ○ |
| | SK 23 | ○ | | SK 23 | ○ | | SK 23 | ○ | |
| | SK 25 | ○ | | SK 25 | ○○○ | | | | |
| | SK 61 | ◉ | | | | | | | |
| | | | | | | | SK 75 | ○ | |
| | SK 104 | | | | | | | | |
| | SK 828 | ○ | | | | | | | |
| | SK 843 | | | SK 843 | ○◉ | | | | |
| *P. boisei* | KNM−ER 6080 | ○ | | | | | | | |
| | KNM−ER 15930 | ◉ | | KNM−ER 15930 | ◉ | | KNM−ER 15930 | ○ | ◉ |
| | | | | KNM−ER 25520 | ○ | | KNM−ER 25520 | ○● | ◉ |
| *A. afarensis* | A.L. 145−35 | | | A.L. 145−35 | ○ | ○ | | | |
| | | | | A.L. 188−1 | ○ | | A.L. 188−1 | ○ | |
| | | | | A.L. 241−14 | | ◉ | | | |
| | A.L. 266−1 | ○ | | A.L. 266−1 | ◉ | | A.L. 266−1 | ○ | |
| | A.L. 288−1 | | | A.L. 288−1 | | | A.L. 288−1 | ○○ | ○ |
| | A.L. 330−5 | | | A.L. 330−5 | | | A.L. 330−5 | ○ | ○ |
| | A.L. 330−7 | | | | | | | | |
| | A.L. 333w−1a | ○ | | A.L. 333w−1a | | | | | |
| | A.L. 417−1a | ○ | | A.L. 417−1a | ○ | | | | |
| | | | | A.L. 440−1 | | | | | |
| | | | | A.L. 443−1 | | | | | |
| *A. africanus* | Sts 9 | | | | | | | | |
| | | | | | | | Sts 59 | ○ | ◉● |
| | | | | StW 3 | ○○◉ | ◉ | | | |
| | StW 145 | | | | | | | | |
| | | | | StW 213 | | | | | |
| | | | | | | | StW 280 | ○◉ | |
| | StW 291 | | | | | | | | |
| | | | | StW 308 | | | | | |
| | StW 309A | | | | | | | | |
| | | | | StW 412A | | ◉ | | | |
| | StW 421A | ○ | | StW 424 | ○ | | | | |
| | | | | StW 491 | ○ | | StW 491 | ○○ | |
| | | | | | | | StW 520 | ◉◉ | |
| | | | | | | | StW 529 | ○ | ◉ |
| | StW 537 | | | StW 537 | | | StW 537 | ○◉ | |
| | | | | StW 560E | ○ | ◉ | StW 560A | ○○ | ○◉ |
| | | | | | | | TM 1520 | ○ | |

DAC: ○ Interconulid type   ◉ Hypoconulid type   ● Entoconid type
LAC: ○ Interconulid type   ◉ Metaconid type   ● Entoconid type

**Figure 6 Number and type of accessory cusps present for each specimen—*Paranthropus* and *Australopithecus*.** Each circle represents a single accessory cusp; specimens with two or three circles in either column display double or triple cusps, respectively. Abbreviations: DAC, Distal accessory cusp; LAC, Lingual accessory cusp.

common in the M₂s and M₃s. Entoconid types are rare; we did not find any among the M₁s or M₂s, and there are only two entoconid types among the M₃s. The two entoconid types are in *H. habilis* and African *H. erectus* M₃s, where there is a fairly even spread between the three types. Metaconid type LACs are the most common type in the M₁s

| | M₁ | DAC | LAC | M₂ | DAC | LAC | M₃ | DAC | LAC |
|---|---|---|---|---|---|---|---|---|---|
| Hominidae gen. et sp. indet. | KNM–ER 5431D | | ◓ | KNM–ER 5431A | | ○ | | | |
| Homo sp. | DNH 67 | | ◓ | | | | | | |
| | SK 15 | ○ ✕ | | SK 15 | ◓ | | SK 15 | ○ | |
| | SK 45 | ✕ | | SK 45 | ◓ | | | | |
| | SKX 258 | | ◓ | | | | | | |
| | StW 80 | | | StW 80 | ◓ | | StW 80 | ✕ | ○ |
| | | | | | | | KNM–ER 1480A | ○○ | ◓ |
| | | | | KNM–ER 1483E | ◓ | | | | |
| | KNM–ER 1802 | | ◓ | KNM–ER 1802 | ○ | | | | |
| | | | | KNM–ER 2597 | ◓ | | | | |
| | | | | | | | KNM–ER 3953 | ○ | ○ |
| | L26–1g | | ◓ | | | | | | |
| H. habilis | KNM–ER 1502 | | ○ | | | | | | |
| | | | | | | | OH 4 | ◓ | ○ |
| | OH 7 | ◓◓ | | OH 7 | ○○ | ○ | | | |
| | OH 13 | ◓ | | | | | OH 13 | ○● | ○ |
| | OH 16 | ◓ | | OH 16 | | ◓ | OH 16 | | ○ |
| | | | | | | | OH 27 | ○◓ | ○ |
| | OMO 75–69–15 | | ◓ | | | | | | |
| | | | | OMO 7–69–19 | | ◓ | OMO 75–69–16 | | ○ |
| African H. erectus | KNM–BK 67 | | ✕ | KNM–BK 67 | | | KNM–BK 67 | | ◓ |
| | KNM–ER 806C | | ◓◓ | KNM–ER 806B | ○ | | KNM–ER 806A | ◓● | |
| | KNM–ER 992A | | ◓ | KNM–ER 992B | ○ | | KNM–ER 992A | | |
| | | | | KNM–ER 1507 | ○ | | | | |
| | | | | KNM–ER 1808G | | | | | |
| | | | | | | | KNM–ER 1812C | ○ | |
| | OH 22 | | | OH 22 | | | | | |
| Asian H. erectus | Sangiran S1b | | ◓ | Sangiran S1b | | | Sangiran S1b | ○ | ○ |
| | | | | Sangiran S7–20 | ○ | | | | |
| | | | | Sangiran S7–42 | | | | | |
| | Sangiran S7–62 | ○○ | ◓ | | | | | | |
| | | | | Sangiran S7–64 | ○ | ○ | | | |
| | | | | Sangiran S7–65 | ◓◓ | ◓ | | | |
| | | | | Sangiran S7–78 | | ○◓ | | | |
| | | | | SMF–8865 | ○ | | | | |
| | CA 804 | ◓◓ | | | | | | | |
| | | | | CA 808 | ◓ | | | | |
| Tighenif | | | | Tighenif 1 | | | Tighenif 1 | | ◓ |
| | Tighenif 2 | | ◓ | Tighenif 2 | ◓ | ○ | Tighenif 2 | ◓ | ○ |

DAC:  ○ Interconulid type  ◓ Hypoconulid type  ● Entoconid type
LAC:  ○ Interconulid type  ◓ Metaconid type  ● Entoconid type

**Figure 7 Number and type of accessory cusps present for each specimen in the sample—*Homo* and KNM-ER 5431 (Hominidae gen. et. sp. indet).** Each circle represents a single accessory cusp; specimens with two or three circles in either column display double or triple cusps, respectively. Areas marked with a red cross are those where part of the specimen was missing such that either the distal or lingual regions could not be scored. Abbreviations: DAC, Distal accessory cusp; LAC, Lingual accessory cusp.

(Table 3) and are confined for this tooth to species in the genus *Homo*. For the M₃s, the interconulid type LAC is most common. Both types are present in the M₂s, but there are more metaconid types overall. There is only one entoconid type LAC, in a M₃ of *A. africanus* (Sts 59).
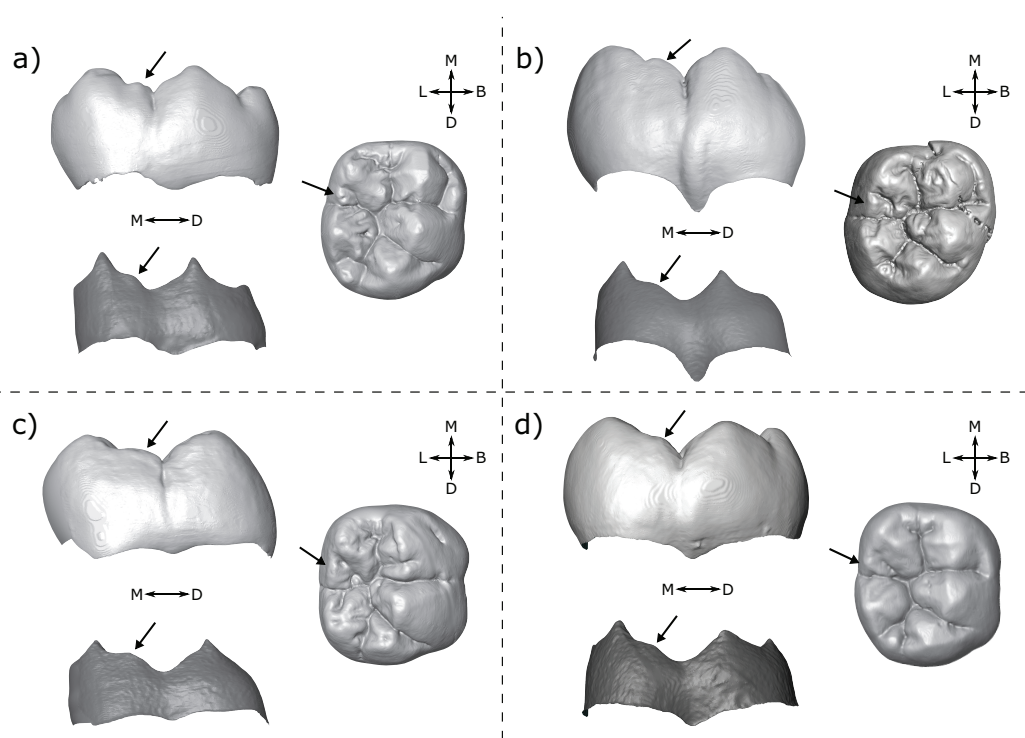
**Figure 8 Shouldering on the distal metaconid ridge.** Shown are four specimens that exhibit shouldering at the EDJ, with variable OES expression. (A) StW 421 RM$_1$—*Australopithecus africanus* (B) SK 104 LM$_1$—*Paranthropus robustus*. Images of this specimen have been reversed for comparative purposes (C) StW 145 RM$_1$—*A. africanus* (D) DNH 60B RM$_1$—*P. robustus*. Each panel shows a lingual view of the OES (top left) and EDJ (bottom left) and an occlusal view of the OES (right). Shouldering features are indicated with arrows, see main text for details. Abbreviations: B, Buccal; L, Lingual; M, Mesial; D, Distal.

The results are summarized graphically in Figs. 6 and 7, including the presence of double and triple accessory cusps. Double LACs are rare but are found in several *Homo* molars. The M$_1$ of OH 7 has a double metaconid type LAC, the only specimen with this arrangement in the sample (present in both antimeres). The M$_1$ of KNM-ER 806 and the M$_2$ Sangiran S7-78 also have double LACs, but in this case one is an interconulid type and the other a metaconid type. Finally, two *A. africanus* M$_3$s have a double LAC. Double DACs are more common. Two Asian *H. erectus* M$_1$s have either a double interconulid type or double hypoconulid type DAC, while numerous M$_2$s and M$_3$s have double DACs, and two M$_2$s have triple DACs (SK 25, *P. robustus* and StW 3, *A. africanus*).

## DISCUSSION

### Shouldering

There are a number of cases in which the morphology at the EDJ differs noticeably from that of the OES. One issue in particular that can be problematic when scoring accessory cusps is shouldering on the marginal ridges associated with the main cusps. This is particularly noticeable on the distal ridge of the metaconid; in lingual view the shoulder is evident at the EDJ as a convexity along the distal marginal ridge (Fig. 8). The OES
manifestation of this shouldering is variable, but the distal ridge of the metaconid is often raised, and in a number of cases there is a fissure present that, together with the lingual groove, appears to demarcate a small or incipient OES cusp. In some cases, this fissure incises the distal ridge of the metaconid such that in lingual view, there appears to be a small cusp present. An example of this is StW 421A (RM$_1$; Fig. 8A), which is described by *Moggi-Cecchi, Grine & Tobias (2006)* as showing an 'incipient postmetaconulid' and given a C7 score of 2 ('small') by *Guatelli-Steinberg & Irish (2005)* using the Arizona State University Dental Anthropology System (ASUDAS; *Turner, Nichol & Scott, 1991*; *Scott & Irish, 2017*). Another example is SK 104 (LM$_1$; Fig. 8B); in this case *Guatelli-Steinberg & Irish (2005)* score the tooth as having no C7, although *Robinson (1956*, p. 103) reports that 13/15 of Swartkrans M$_1$s described display a 'lingual accessory cusp partially separated from the distal portion of the metaconid'. It is not clear if SK 104 is one of these specimens, but it is likely given that there are a number of molars in this sample with weaker expressions of this feature. In other specimens, the secondary fissure does not incise the distal metaconid ridge. In these cases, the shape of the distal ridge of the metaconid at the OES mirrors that of the EDJ in that it is raised and somewhat concave in shape. However, in occlusal view, the fissure still suggests the presence of a cusp. Examples of this are StW 145 (RM$_1$; Fig. 8C); scored by *Guatelli-Steinberg & Irish (2005)* as having a medium sized C7 (ASUDAS score 3), and DNH 60B (RM$_1$; Fig. 8D); described by *Moggi-Cecchi et al. (2010)* as showing an 'incipient post-metaconulid'.

Shouldering is not limited to the lower molars. *Martin et al. (2017)* outlined a similar trait in modern human and Neanderthal upper molars when describing the feature they term the 'post-paracone tubercle'. In some cases, this refers to a distinct cusp on the paracone distal ridge, however in others there was only shouldering on the ridge, similar to a number of the cases outlined here. This was also found to be present in other hominoid taxa by *Ortiz et al. (2017)*, who suggested that these examples of shouldering represent a minor expression of the post-paracone tubercle trait.

The phenomenon of shouldering raises important questions about the developmental nature of accessory cusps. Epithelial signalling centres called enamel knots have a controlling role in cusp patterning during tooth development. The primary enamel knot forms first, at the tip of the developing tooth bud, followed by secondary enamel knots, at the future position of each cusp. The formation of these secondary enamel knots directs folding of the inner enamel epithelium, the future boundary between enamel and dentine, at the site of each cusp. We should therefore expect that all true accessory cusps are initiated by the presence of a secondary enamel knot. If so, are secondary enamel knots capable of producing broad shoulder-like features such as those outlined above? This question is important because if shouldering features were not initiated by enamel knots, then they would not be developmentally homologous to accessory cusps, and may need to be considered separately in studies of taxonomy or phylogeny. An interesting example is KNM-ER 806, for which the M$_3$ antimeres differ in LAC expression (Fig. 9). The left M$_3$ has a broad shouldered distal metaconid ridge with no clear cusp, while the right M$_3$ has a distinct cusp on the distal metaconid ridge. This could lend support to the idea that shouldering is equivalent to minor expression of an accessory cusp, with
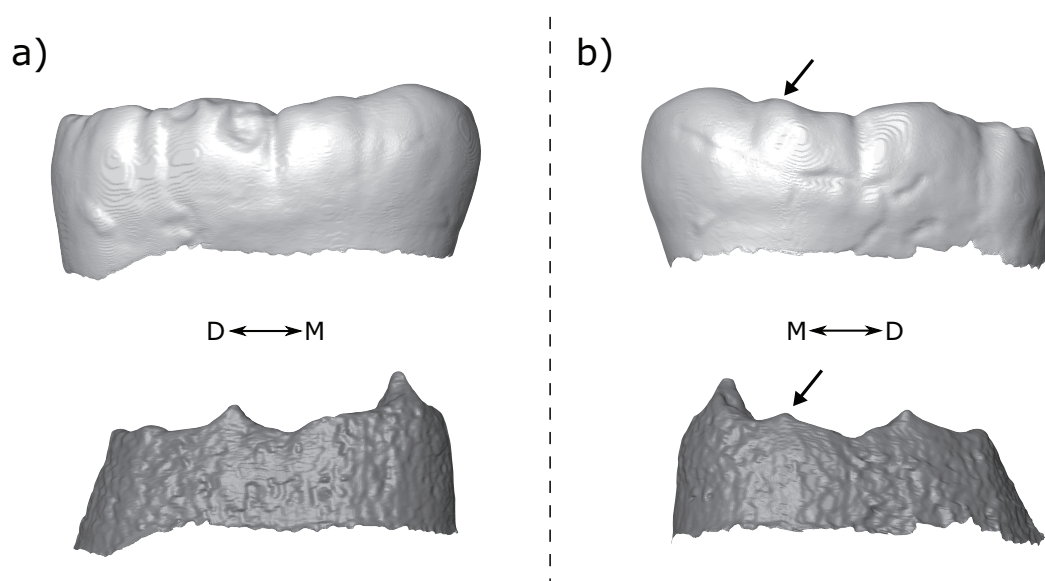
**Figure 9  Third mandibular molar antimeres of KNM-ER 806—*Homo erectus*.** (A) KNM- ER 806A—Left $M_3$ shows broad shouldering on the distal metaconid ridge. (B) KNM- ER 806C—Right $M_3$ shows a clear metaconid type lingual accessory cusp. Both panels show the specimens in lingual view at the OES (top) and EDJ (bottom). Accessory cusps are indicated with arrows. Abbreviations: M, Mesial; D, Distal.
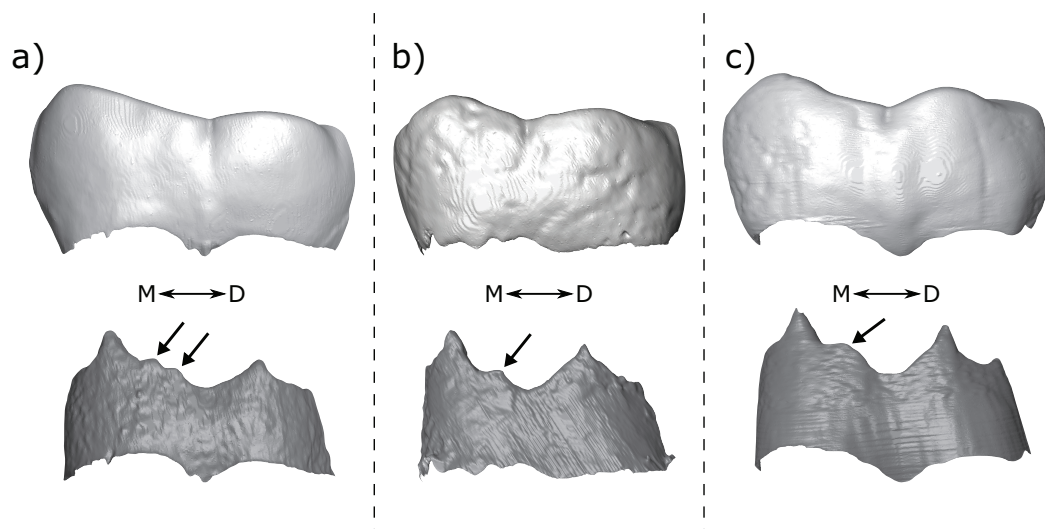
**Figure 10  *Homo habilis* $M_1$s from Olduvai Gorge.** Shown are three Olduvai *H. habilis* lower first molars. All exhibit cusp features on the distal ridge of the metaconid, but the form is different in each. (A) OH 7 $LM_1$ showing two small, distinct accessory cusps on the distal ridge of the metaconid. Images of this specimen have been reversed for comparative purposes. (B) OH 13 $RM_1$ showing a single small accessory cusp on the distal ridge of the metaconid. (C) OH 16 $RM_1$ showing a single broad accessory cusp. Each panel shows the specimens in lingual view at the OES (top) and EDJ (bottom). Accessory cusps are indicated with arrows. Abbreviations: M, Mesial; D, Distal.

the right $M_3$ showing slightly stronger accessory cusp expression than the left. Furthermore, if shouldering and cusps represent differing degrees of expression of the same trait, then, at least to some extent, they are independent of size given that specimens may have very large shouldering features (Figs. 8C, 9A) or very small, but distinct, accessory cusps (Figs. 10A, 10B).

Ultimately, we need a better understanding of the developmental basis of shouldering in order to determine the relationship between shouldering features and accessory cusps. In the short term, a scheme that includes shouldering within the definition of the LAC, but scores it separately to clear and distinct cusps, would be useful as it would allow these traits to be assessed either separately or together, and would allow us to reassess these data if our understanding of the development of these traits improves. However, this brings practical difficulties; there are a wide array of morphologies that could be considered as examples of shouldering, including some that are subtle and difficult to score reliably. In the present study we scored only cusps that either have a clear apex, or are raised above the level of the marginal ridge on both sides, thereby excluding the majority of examples of shouldering (although some cusps that fit this definition, such as the right $M_1$ of OH 16, Fig. 10C, also resemble shouldering features). An alternative solution would be to conduct geometric morphometric analysis of the marginal ridge between the metaconid and entoconid. This would remove the need for discrete trait categories, instead measuring the shape of any cusp or shouldering feature without making assumptions about their developmental underpinnings.

## Cusps present only at the outer enamel surface

Another issue relates to the correspondence between the EDJ and OES. In some cases, there appears to be a cusp at the OES with no clear corresponding EDJ feature. This can be present lingually or distally, although there are more examples on the distal marginal ridge in our sample. In some cases, particularly in scans exhibiting poor tissue distinction, it is possible that the corresponding cusp at the EDJ is too small to be distinguished. This may be particularly problematic in third molars since the cusps are generally smaller, and some accessory cusps are represented by very low dentine horns at the EDJ. However, there are a number of examples of this phenomenon in specimens with good tissue distinction, and in first and second molars also (Fig. 11). These examples generally involve quite small cusps, however they are large enough to be noted as accessory cusps; all of the specimens shown in Fig. 11 have been described as having an accessory cusp/cuspule at the OES (*Johanson et al., 1982*; *Moggi-Cecchi, Grine & Tobias, 2006*; *Moggi-Cecchi et al., 2010*; *Robinson, 1956*).

It is not clear why the EDJ does not show any evidence of a dentine horn in these examples. However, in some cases (Figs. 11B–11D) it does appear that regions of the EDJ marginal ridges that we would expect to be concave, are instead flat. Given that we have a number of cases in which dentine horns are low and broad, it is possible that the presence of an elevation of the marginal ridge between main cusps (like for the shouldering but in the interconulid region) could generate a portion of the EDJ that looks flat, but

none
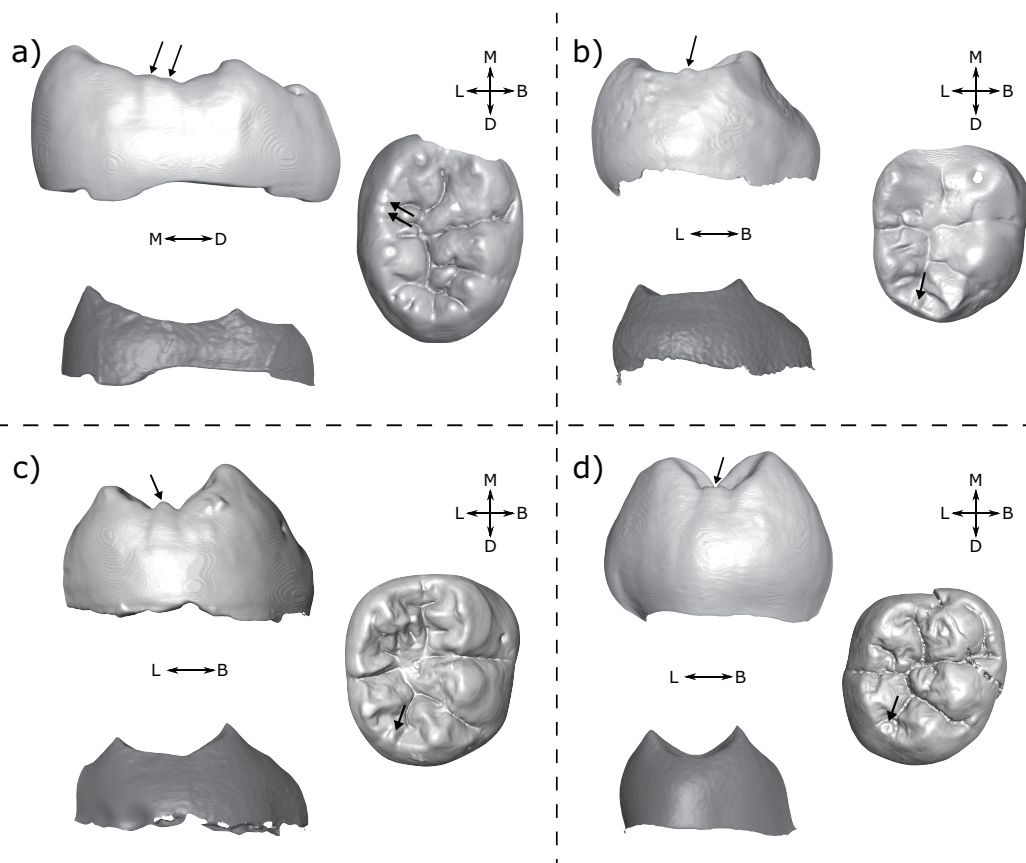
**Figure 11 Specimens displaying cusps at the OES but not at the EDJ.** (A) DNH 75 LM$_3$ (*Paranthropus robustus*) displays two small cusps on the lingual marginal ridge at the OES. Left: lingual view of the OES (top) and EDJ (bottom); Right: occlusal view of the OES. (B) A.L. 288-1 RM$_2$ (*Australopithecus afarensis*) with a small tubercle on the distal marginal ridge; Left: distal view at the OES (top) and EDJ (bottom); Right: occlusal view of the OES. (C) StW 421A RM$_2$ (*Australopithecus africanus*) shows a clear small cusp on the distal marginal ridge. Left: lingual view of the OES (top) and EDJ (bottom); Right: occlusal view of the OES. (D) SK 104 LM$_1$ (*P. robustus*) shows a small cusp on the distal marginal ridge; Left: distal view at the OES (top) and EDJ (bottom); Right: occlusal view of the OES. OES cusps are marked with arrows. Images in (A) and (D) have been reversed for comparative purposes. Abbreviations: B, Buccal; L, Lingual; M, Mesial; D, Distal.

is in fact raised above the level that it otherwise would be, if this dentine horn-like feature was not present. This flat morphology may then be exaggerated by the processes of enamel deposition and appear as a small cuspule at the OES. Modelling on pig teeth has suggested that concave and convex EDJ features can have different effects on enamel deposition, which is suggested to explain how small differences in EDJ topography can correspond to large differences at the OES (*Häkkinen et al., 2019*). Interestingly however, this process does not require the presence of an enamel knot, meaning that some features that appear as cusps at the OES may simply derive from small ridges at the EDJ. This process could also explain the presence of cusp-like OES features overlying shouldering at the EDJ as outlined above. In both cases, the absence of an enamel knot would mean these features are not developmentally homologous to true accessory cusps (i.e. those initiated by an enamel knot).
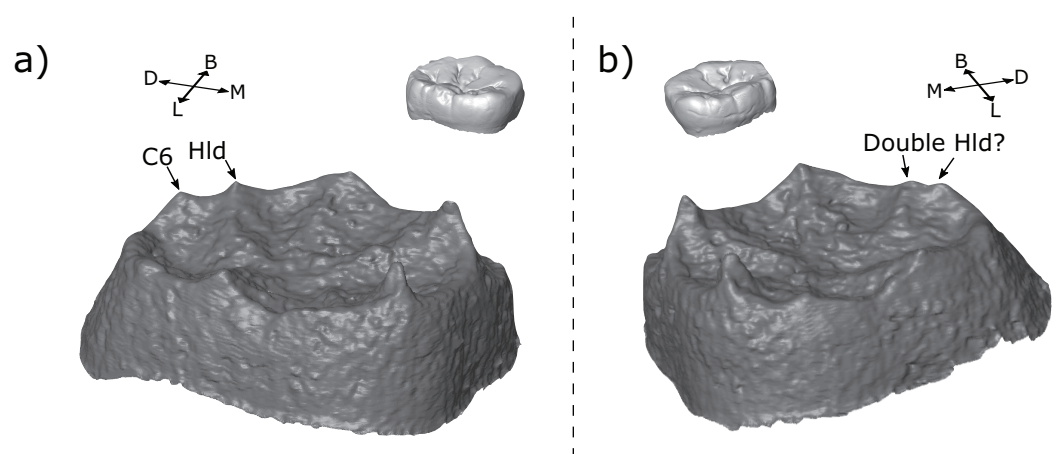
**Figure 12 Left and right antimeres of KNM-ER 806 (*Homo erectus*) third molars.** (A) The left M₃ shows a hypoconulid with a hypoconulid type distal accessory cusp. (B) The right M₃ shows an apparently double hypoconulid. Specimens are shown in oblique view at the EDJ (bottom) and OES (top—thumbnail). Abbreviations: B, Buccal; L, Lingual; M, Mesial; D, Distal; Hld, Hypoconulid.

Alternatively, it is possible that secondary enamel knots induce ameloblasts to deposit more enamel in cuspal regions than in adjacent regions of the crown. In this case, late forming secondary enamel knots, whose effect on the inner enamel epithelium may be very minor or nonexistent, may still produce noticeable cusps at the OES through the effect of differential enamel deposition in these regions. This mechanism was previously put forward in *Skinner et al. (2008)* but remains to be tested.

## Twinned dentine horns

Another interesting phenomenon is that of twin dentine horns. *Martin et al. (2017)* noted the presence of this feature in Neanderthal maxillary and mandibular molars, and *Davies et al. (2019)* suggested that some mandibular premolars display a similar feature on the protoconid. Twinned dentine horns are interesting because the patterning cascade model of cusp development predicts that enamel knots should be inhibited from forming in the immediate vicinity of one another (*Jernvall, 2000*; *Jernvall & Thesleff, 2000*), suggesting that twinned dentine horns may result from a single enamel knot, rather than two separate enamel knots. A similar argument could be made of double accessory cusps forming in the immediate vicinity of each other as we see in the M₁s of OH 7 (Fig. 10A).

There is a small number of possible examples of the twinned dentine horns trait in our sample on the metaconid or hypoconulid. The most striking example is seen in the M₃ antimeres of KNM-ER 806 (Fig. 12). If the two teeth were scored in isolation, we would suggest that the LM₃ has a single hypoconulid dentine horn and a hypoconulid type DAC, while the RM₃ has double hypoconulid dentine horn. Both antimeres have two dentine horns in the distolingual margin of the tooth; the only discernable difference between them is the distance between the two dentine horns; in one case small enough to be considered a double cusp and in the other large enough for one to be considered an accessory cusp. This would seem to suggest that both traits are the result of the same
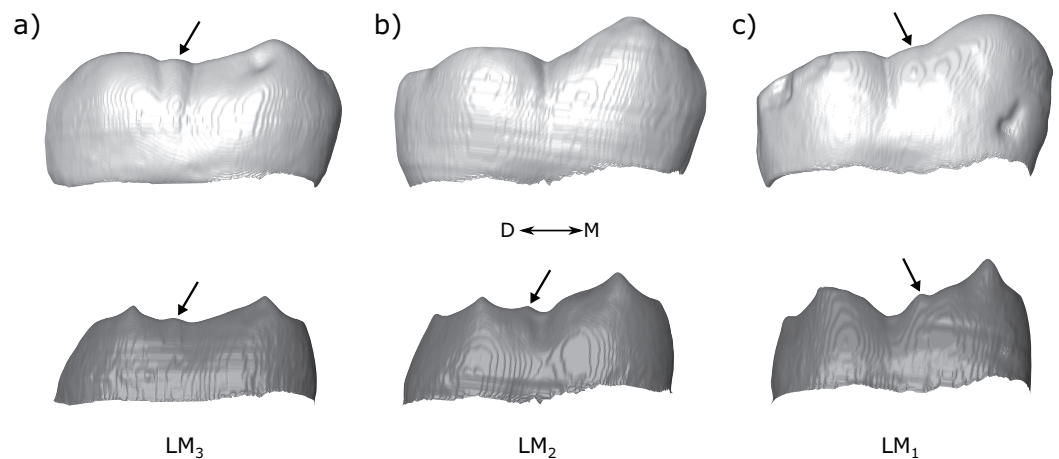
**Figure 13 Molar row of Tighenif 2.** The left molars of Tighenif 2 are shown at the OES and EDJ, showing the position of the LAC along the tooth row. Molars are shown in lingual view; (A) $LM_3$, (B) $LM_2$, and (C) $LM_1$. Arrows indicate the position of the accessory cusps. Note that the accessory cusp is not visible at the OES of the $LM_2$ (B) due to occlusal wear. Abbreviations: M, Mesial; D, Distal.

developmental processes, with minor differences during development leading to the observed differences in spacing. In this case, it would suggest that either: (1) twinned dentine horns can, in some cases, appear with a larger distance between the tips than previously recognized, or (2) accessory cusps can appear very close to the main cusp in some cases. Either scenario questions our ability to reliably tell the difference between the two traits, if they are indeed distinct traits. Alternatively, we may conclude that the two antimeres simply show different morphologies. Few antimeres were included in this study, but they have been useful in investigating developmental questions; we suggest that future studies include both antimeres whenever possible.

## Accessory cusp types

In this study, we distinguished between several types of DACs (Fig. 2) and LACs (Fig. 3) based on the association between accessory cusps and the main cusps. We found that the majority of DACs are of the interconulid type, followed by hypoconulid type, although these are more common in $M_2$s and $M_3$s than in $M_1$s. For the LACs, the majority were found to be metaconid types overall, although there were progressively more interconulid types moving posteriorly along the tooth row. It should be noted that in $M_3$s the cusps are often very low, meaning the mesial and distal ridges of the main cusps are less steep and it is harder to distinguish between the different types. We would expect this to increase the number of interconulid types since any accessory cusps not clearly associated with a main cusp were designated as interconulid types. This may explain the increased number of interconulid type LACs along the tooth row.

Some authors distinguish a 'postmetaconulid' as distinct from a 'C7' (*Grine et al., 2019*; *Kaifu, Aziz & Baba, 2005*; *Moggi-Cecchi, Grine & Tobias, 2006*; *Skinner et al., 2020*; *Suwa, Wood & White, 1994*). Given that we did not find any clear taxon-specific patterns when the distal and lingual accessory cusps were broken down into types that were not

present in the pooled samples, as well as the difficulty in distinguishing between the types at the OES, we suggest that these distinctions are likely not useful for taxonomic studies. The types described here may be useful in descriptions of dental material, although it is unclear whether the types we distinguish here represent distinct traits; it is more likely that there is a continuous variation in accessory cusp placement, and that this variation is only partly captured by the categories used here. A good example illustrating this is the molar row of Tighenif 2 (Fig. 13; see also *Zanolli & Mazurier, 2013*). All three molars have a LAC, but its position shifts distally along the molar row from a clear metaconid type in the $M_1$, to interconulid types in the $M_2$ and $M_3$ that are situated close to the entoconid (the LACs in the $M_2$ and $M_3$ are not situated on the mesial ridge of the entoconid, which would make them an entoconid type, but they are situated close to the entoconid because the cusp is low and its mesial ridge does not extend very far mesially on the crown). If the variation in accessory cusp placement is continuous, then a method of recording this variation continuously might better capture metameric differences, or provide better taxonomic discrimination, than the categories used here.

Finally, it is interesting to note that there are very few accessory cusps closely associated with the entoconid, either DACs or LACs. We find only three examples, all in $M_3$s. It is not clear why accessory cusps are less likely to form in this region, although in the case of the LAC, the entoconid is typically initiated later than the metaconid (*Smith et al., 2007*; *Mahoney, 2008*), and the mesial entoconid ridge is usually much shorter than the distal metaconid ridge, suggesting there is less time and space for accessory cusps to form in this region. In the case of the DAC, the mechanism is less clear since the hypoconulid is frequently the smallest cusp, and is thought to be the last to initiate, but we find that hypoconulid type DACs are nonetheless fairly common.

## Use of accessory cusps for taxonomy

We find that there are a number of patterns present in accessory cusp expression that may be useful in differentiating between hominin taxa. We find that *Paranthropus* molars tend to have DACs but no LACs, consistent with studies of the OES (*Suwa, White & Howell, 1996*; *Suwa, Wood & White, 1994*; *Wood & Abbott, 1983*). *Guatelli-Steinberg & Irish (2005)* reported a comparably high DAC frequency at the OES for *A. afarensis* and *P. robustus*. Our results, consistent with other studies of the OES (*Bailey & Wood, 2007*; *Suwa, Wood & White, 1994*), instead suggest DACs are less frequent in *A. afarensis*. *Kimbel & Delezene (2009)* suggested that *A. afarensis* $M_3$s often have a double DAC at the OES, distinguishing the species from *Paranthropus* and *Homo*. But we find double DACs in the $M_3$s of *A. afarensis, A. africanus, P. robustus, P. boisei, Homo* sp., *H. habilis* and African *H. erectus*. In *A. africanus* they are particularly frequent (5/8). For the most part, we suggest that accessory cusps in the $M_3$s are too variable to be taxonomically informative. We also find support for the suggestion that LACs are more common in non-robust taxa (*Suwa, Wood & White, 1994*; *Wood & Abbott, 1983*). In particular, LACs are associated with early *Homo* at the EDJ (*Ortiz et al., 2017*), and the presence of LACs at the OES have been used to support an assignment of a number of specimens to *Homo*

(*Braga & Thackeray, 2003*; *Grine, 1989*; *Villmoare et al., 2015*; *Wood, 1991*). We find that LACs are frequent in *Homo* molars overall, but this is particularly true of *H. habilis*.

However, there are also some differences in the frequencies reported here from those reported in various studies of the OES (*Bailey & Wood, 2007*; *Guatelli-Steinberg & Irish, 2005*; *Irish et al., 2018*; *Suwa, White & Howell, 1996*; *Suwa, Wood & White, 1994*; *Wood & Abbott, 1983*). These differences may be due to differing study samples, or grouping of specimens, or they may be the result of some of the issues described above such as shouldering of the distal marginal ridges or OES cusps with minimal EDJ expression. However, there are also differences likely to be introduced through the scoring systems employed. A number of studies utilize ASUDAS accessory cusp traits with a presence/ absence breakpoint. For example, *Irish et al. (2018)* score the presence of a C7 with a breakpoint of 2, meaning that a tooth scored as 1 or 1A in this system is counted as absent. Types 1 and 1A refer to a "small, wedge-shaped cusp", or a "groove on the lingual surface of the metaconid", respectively (*Scott & Irish, 2017*, p. 219). It is likely that a number of the specimens that we score as having a LAC present at the EDJ could be scored for the C7 ASUDAS trait as 1 or 1A at the OES, or in some cases even as 0. Good examples of this are teeth with small metaconid type LACs; with moderate levels of dental wear, all that remains of this feature at the OES is a small fissure. This may explain why, for example, we report higher frequencies of LAC presence in *H. habilis* than *Irish et al. (2018)* at the OES.

Beyond the issues presented above, there are also some fundamental questions surrounding the use of accessory cusps in studies of taxonomy. Our understanding of tooth development suggests that accessory cusps are not individually patterned. Instead, according to the patterning cascade model (*Jernvall, 2000*; *Jernvall & Thesleff, 2000*), accessory cusp formation is dependent on the size and spacing of earlier forming cusps. This means that rather than accessory cusps representing a primary trait, they are dependent on the shape of the crown, the size and spacing of the primary cusps, and that of earlier forming accessory cusps. The taxonomic signal present in accessory cusps, as reported here and elsewhere (*Suwa, White & Howell, 1996*; *Wood & Abbott, 1983*; *Ortiz et al., 2017*), may come from the fact that the size and spacing factors they depend on are genetically determined, or that these factors are themselves dependent on further upstream genetically determined factors. Equally, this may make accessory cusps particularly liable to homoplasy. Tooth shape, as well as cusp size and spacing factors, are variable in hominin teeth, and multiple arrangements of these factors could lead to the development of accessory cusps in separate hominin lineages. In this case, it would be preferable to analyze these size and spacing factors directly through measures of crown shape, relative cusp areas or geometric morphometric analysis of crown shape, either at the OES or at the EDJ.

The factors controlling accessory cusp formation are complex and not fully understood. For example, it is not clear how double or triple accessory cusps form. We may expect that in some cases there may be enough space available on the lingual or distal marginal ridges for multiple accessory cusps to form, however we would expect them to be

relatively well-spaced apart, which is not always the case (e.g. OH 7 $M_1$; Fig. 10A). It may be possible that these cases of closely spaced accessory cusps are caused by the same (unknown) processes responsible for the twinned dentine horns that sometimes underly the main cusps, as outlined above. If this were the case, they would have to be distinguished from double accessory cusps that are well-spaced from each other. It is also unclear which conditions lead to multiple accessory cusps forming as opposed to a single large accessory cusp. Trait scoring systems such as the ASUDAS score accessory cusps according to size (although a DAC can alternatively be scored using the 'cusp number' trait, in which case it is only present or absent). This relies on the assumption that a larger cusp represents a greater level of expression of the trait. Equally, it could be argued that a double or triple accessory cusp arrangement is equivalent to greater expression of the trait, particularly if the 'trait' in question is actually a combination of size and spacing factors that permit the development of accessory cusp(s). The ASUDAS system does not ordinarily score the presence of double/triple accessory cusps, although some authors have added or adapted traits for multiple DACs (*Bailey & Wood, 2007*; *Irish et al., 2018*). However, for the most part, a specimen displaying multiple small DACs or LACs would presumably be scored as having a small accessory C6 or C7, a minor expression of the trait.

## CONCLUSION

We find that there are a number of patterns in lower molar accessory cusp expression at the EDJ. *Paranthropus robustus* $M_1$s and $M_2$s very often have a DAC and no LAC, and no LACs were found in any *Australopithecus* or *Paranthropus* $M_1$s. *Homo habilis* $M_1$s and $M_2$s very often combine the absence of a DAC with the presence of a LAC. However, the EDJ also reveals a high level of complexity in accessory cusp expression that is not always visible at the OES. Cusp-like morphologies at the OES may, at the EDJ, be represented by one or more dentine horns, or by a shouldering on the marginal ridge of one of the main cusps, or seemingly by nothing at all. We therefore suggest that, where possible, accessory cusps are assessed at the EDJ as well as the OES. Even so, our understanding of the development of these traits is poor and we cannot be sure they are generated by the same developmental mechanisms in all cases. Further, our understanding of the development of accessory cusps suggests that they are dependent on a number of factors such as the size and spacing of earlier forming cusps and the space available on the crown, suggesting it may be preferable to analyze these factors directly.

## ACKNOWLEDGEMENTS

For access to specimens and microCT scans, we would like to thank Bernhard Zipfel, Sifelani Jira (Evolutionary Studies Institute, University of the Witwatersrand), Miriam Tawane (Ditsong Museum), Emma Mbua and Job Kibii (National Museums of Kenya), Audax Mabulla (National Museum of Tanzania), the Tanzania Commission for Science and Technology, Metasebia Endalemaw, Yared Assefa (Ethiopian Authority for Research and Conservation of Cultural heritage), Christine Argot and Hervé Lelièvre (Muséum national d'Histoire naturelle), Roberto Macchiarelli (University of Poitiers and Muséum national d'Histoire naturelle) and Arnaud Mazurier (University of Poitiers),

Friedemann Schrenk and Christine Hemm (Senckenberg Research Institute and Natural History Museum Frankfurt). We express our gratitude to the Werner Reimers Foundation in Bad Homburg, which provides the Gustav Heinrich Ralph von Koenigswald collection of fossil hominids as a permanent loan for scientific research to the Senckenberg Research Institute and Natural History Museum Frankfurt. For scanning and technical assistance, we thank Kudakwashe Jakata, Arnaud Mazurier, Burkhard Schillinger, David Plotzki and Heiko Temming. For segmentation and imaging assistance, we thank Lia Schurtenberger and Paulina Dittmann.

### Funding

This work was funded by the Max Planck Society and the European Research Council (ERC) under the European Union's Horizon 2020 Research and Innovation Programme (grant agreement No. 819960). The funders had no role in study design, data collection and analysis, decision to publish, or preparation of the manuscript.

### Grant Disclosures

The following grant information was disclosed by the authors:
Max Planck Society and the European Research Council (ERC).
European Union's Horizon 2020 Research and Innovation Programme: 819960.

### Competing Interests

The authors declare that they have no competing interests.

### Author Contributions

- Thomas W. Davies conceived and designed the experiments, performed the experiments, analyzed the data, prepared figures and/or tables, authored or reviewed drafts of the paper, and approved the final draft.
- Zeresenay Alemseged conceived and designed the experiments, performed the experiments, authored or reviewed drafts of the paper, and approved the final draft.
- Agness Gidna conceived and designed the experiments, performed the experiments, authored or reviewed drafts of the paper, and approved the final draft.
- Jean-Jacques Hublin conceived and designed the experiments, performed the experiments, authored or reviewed drafts of the paper, and approved the final draft.
- William H. Kimbel conceived and designed the experiments, performed the experiments, authored or reviewed drafts of the paper, and approved the final draft.
- Ottmar Kullmer conceived and designed the experiments, performed the experiments, authored or reviewed drafts of the paper, and approved the final draft.
- Fred Spoor conceived and designed the experiments, performed the experiments, authored or reviewed drafts of the paper, and approved the final draft.
- Clément Zanolli conceived and designed the experiments, performed the experiments, analyzed the data, authored or reviewed drafts of the paper, and approved the final draft.

Peer

- Matthew M. Skinner conceived and designed the experiments, performed the experiments, analyzed the data, prepared figures and/or tables, authored or reviewed drafts of the paper, and approved the final draft.

## Data Availability

The accessory cusp scores for the sample are available in Table S1. The images and descriptions of each specimen are available in the Supplemental File.

The scan data used in this study is curated by the museums and institutes who curate the original fossil material. The following people should be contacted for inquiries about access to fossils:

For specimens from Olduvai Gorge, Agness Gidna (National Museum of Tanzania), for specimens from Koobi Fora, Ileret and Baringo, Job Kibii (National Museums of Kenya), for specimens from Sterkfontein, Bernhard Zipfel (Evolutionary Studies Institute, University of the Witwatersrand), for specimens from Drimolen and Swartkrans, Miriam Tawane (Ditsong Museum), for specimens from Hadar and Omo, Metasebia Endalemaw and Yared Assefa (Ethiopian Authority for Research and Conservation of Cultural heritage), for specimens from Tighenif, Christine Argot (Muséum national d'Histoire naturelle) and for specimens from Sangiran and the Chinese Apothecary collection, Ottmar Kullmer (Senckenberg Research Institute and Natural History Museum Frankfurt).

## Supplemental Information

Supplemental information for this article can be found online at http://dx.doi.org/10.7717/peerj.11415#supplemental-information.

## REFERENCES

**Bailey SE, Wood BA. 2007.** Trends in postcanine occlusal morphology within the hominin clade: the case of *Paranthropus*. In: Bailey SE, Hublin JJ, eds. *Dental Perspectives on Human Evolution: State of the Art Research in Dental Paleoanthropology*. Dordrecht: Springer, 33–52.

**Braga J, Thackeray JF. 2003.** Early *Homo* at Kromdraai B: probabilistic and morphological analysis of the lower dentition. *Comptes Rendus Palevol* **2(4)**:269–279 DOI 10.1016/S1631-0683(03)00044-7.

**Burnett S, Irish J, Fong M. 2013.** Wears the problem—examining the effect of dental wear on studies of crown morphology. In: Scott GR, Irish JD, eds. *Anthropological Perspectives on Tooth Morphology*. Camridge: Cambridge University Press, 535–554.

**Davies TW, Delezene LK, Gunz P, Hublin J-J, Berger LR, Gidna A, Skinner MM. 2020.** Distinct mandibular premolar crown morphology in *Homo naledi* and its implications for the evolution of Homo species in southern Africa. *Scientific Reports* **10(1)**:1–13 DOI 10.1038/s41598-019-56847-4.

**Davies TW, Delezene LK, Gunz P, Hublin JJ, Skinner MM. 2019.** Endostructural morphology in hominoid mandibular third premolars: discrete traits at the enamel-dentine junction. *Journal of Human Evolution* **136**:102670 DOI 10.1016/j.jhevol.2019.102670.

**Fiorenza L, Menter CG, Fung S, Lee J, Kaidonis J, Moggi-Cecchi J, Townsend G, Kullmer O. 2020.** The functional role of the Carabelli trait in early and late hominins. *Journal of Human Evolution* **145**:102816 DOI 10.1016/j.jhevol.2020.102816.

**Grine FE. 1984.** The deciduous dentition of the Kalahari San, the South African Negro and the South African Plio-Pleistocene Hominids. Ph.D. Dissertation, University of the Witwatersrand.

**Grine FE. 1989.** New hominid fossils from the Swartkrans formation (1979–1986 excavations): craniodental specimens. *American Journal of Physical Anthropology* **79(4)**:409–449 DOI 10.1002/ajpa.1330790402.

**Grine F, Franzen J. 1994.** Fossil hominid teeth from the Sangiran Dome (Java, Indonesia). *Courier Forschungsinstitut Senckenberg* **171**:75–103.

**Grine FE, Leakey MG, Gathago PN, Brown FH, Mongle CS, Yang D, Jungers WL, Leakey LN. 2019.** Complete permanent mandibular dentition of early *Homo* from the upper Burgi Member of the Koobi Fora Formation, Ileret, Kenya. *Journal of Human Evolution* **131**:152–175 DOI 10.1016/j.jhevol.2019.03.017.

**Guatelli-Steinberg D, Irish JD. 2005.** Brief communication: early hominin variability in first molar dental trait frequencies. *American Journal of Physical Anthropology* **128(2)**:477–484 DOI 10.1002/ajpa.20194.

**Hunter JP, Guatelli-Steinberg D, Weston TC, Durner R, Betsinger TK. 2010.** Model of tooth morphogenesis predicts Carabelli cusp expression, size, and symmetry in humans. *PLOS ONE* **5(7)**:e11844 DOI 10.1371/journal.pone.0011844.

**Häkkinen TJ, Sova SS, Corfe IJ, Tjäderhane L, Hannukainen A, Jernvall J. 2019.** Modeling enamel matrix secretion in mammalian teeth. *PLOS Computational Biology* **15(5)**:e1007058 DOI 10.1371/journal.pcbi.1007058.

**Irish JD, Bailey SE, Guatelli-Steinberg D, Delezene LK, Berger LR. 2018.** Ancient teeth, phenetic affinities, and African hominins: another look at where *Homo naledi* fits in. *Journal of Human Evolution* **122**:108–123 DOI 10.1016/j.jhevol.2018.05.007.

**Jernvall J. 2000.** Linking development with generation of novelty in mammalian teeth. *Proceedings of the National Academy of Sciences of the United States of America* **97(6)**:2641–2645 DOI 10.1073/pnas.050586297.

**Jernvall J, Thesleff I. 2000.** Reiterative signaling and patterning during mammalian tooth morphogenesis. *Mechanisms of Development* **92(1)**:19–29 DOI 10.1016/S0925-4773(99)00322-6.

**Johanson DC, Lovejoy CO, Kimbel WH, White TD, Ward SC, Bush ME, Latimer BM, Coppens Y. 1982.** Morphology of the Pliocene partial hominid skeleton (AL 288-1) from the Hadar formation, Ethiopia. *American Journal of Physical Anthropology* **57(4)**:403–451 DOI 10.1002/ajpa.1330570403.

**Johanson DC, White TD, Coppens Y. 1982.** Dental remains from the Hadar formation, ethiopia: 1974–1977 collections. *American Journal of Physical Anthropology* **57(4)**:545–603 DOI 10.1002/ajpa.1330570406.

**Kaifu Y, Aziz F, Baba H. 2005.** Hominid mandibular remains from Sangiran: 1952–1986 collection. *American Journal of Physical Anthropology* **128(3)**:497–519 DOI 10.1002/ajpa.10427.

**Kimbel WH, Delezene LK. 2009.** Lucy redux: a review of research on *Australopithecus afarensis*. *American Journal of Physical Anthropology* **140(S49)**:2–48 DOI 10.1002/ajpa.21183.

**Le Cabec A, Dean MC, Begun DR. 2017.** Dental development and age at death of the holotype of *Anapithecus hernyaki* (RUD 9) using synchrotron virtual histology. *Journal of Human Evolution* **108**:161–175 DOI 10.1016/j.jhevol.2017.03.007.

**Mahoney P. 2008.** Intraspecific variation in M1 enamel development in modern humans: implications for human evolution. *Journal of Human Evolution* **55(1)**:131–147 DOI 10.1016/j.jhevol.2008.02.004.

**Martin RM, Hublin J-J, Gunz P, Skinner MM. 2017.** The morphology of the enamel-dentine junction in Neanderthal molars: gross morphology, non-metric traits, and temporal trends. *Journal of Human Evolution* **103**:20–44 DOI 10.1016/j.jhevol.2016.12.004.

**Martinón-Torres M, De Castro JMB, De Pinillos MM, Modesto-Mata M, Xing S, Martín-Francés L, García-Campos C, Wu X, Liu W. 2019.** New permanent teeth from Gran Dolina-TD6 (Sierra de Atapuerca): the bearing of *Homo antecessor* on the evolutionary scenario of Early and Middle Pleistocene Europe. *Journal of Human Evolution* **127**:93–117 DOI 10.1016/j.jhevol.2018.12.001.

**Moggi-Cecchi J, Grine FE, Tobias PV. 2006.** Early hominid dental remains from Members 4 and 5 of the Sterkfontein formation (1966–1996 excavations): catalogue, individual associations, morphological descriptions and initial metrical analysis. *Journal of Human Evolution* **50(3)**:239–328 DOI 10.1016/j.jhevol.2005.08.012.

**Moggi-Cecchi J, Menter C, Boccone S, Keyser A. 2010.** Early hominin dental remains from the Plio-Pleistocene site of Drimolen, South Africa. *Journal of Human Evolution* **58(5)**:374–405 DOI 10.1016/j.jhevol.2010.01.006.

**Moormann S, Guatelli-Steinberg D, Hunter J. 2013.** Metamerism, morphogenesis, and the expression of Carabelli and other dental traits in humans. *American Journal of Physical Anthropology* **150(3)**:400–408 DOI 10.1002/ajpa.22216.

**Nager G. 1960.** Der Vergleich zwischen dem raumlichen Verhalten des Dentinkronenreliefs und dem Schmelzrelief der Zahnkrone. *Acta Anatomica* **42(3)**:226–250 DOI 10.1159/000141662.

**Ortiz A, Bailey SE, Hublin JJ, Skinner MM. 2017.** Homology, homoplasy and cusp variability at the enamel-dentine junction of hominoid molars. *Journal of Anatomy* **231(4)**:585–599 DOI 10.1111/joa.12649.

**Ortiz A, Bailey SE, Schwartz GT, Hublin J-J, Skinner MM. 2018.** Evo-devo models of tooth development and the origin of hominoid molar diversity. *Science Advances* **4(4)**:eaar2334 DOI 10.1126/sciadv.aar2334.

**Robinson JT. 1956.** *The dentition of Australopithecinae.* Pretoria: Transvaal Museum.

**Scott GR, Irish JD. 2017.** *Human tooth crown and root morphology: the Arizona State University Dental Anthropology system.* Cambridge: Cambridge University Press.

**Skinner MM, De Vries D, Gunz P, Kupczik K, Klassen RP, Hublin J-J, Roksandic M. 2016.** A dental perspective on the taxonomic affinity of the Balanica mandible (BH-1). *Journal of Human Evolution* **93**:63–81 DOI 10.1016/j.jhevol.2016.01.010.

**Skinner MM, Gunz P. 2010.** The presence of accessory cusps in chimpanzee lower molars is consistent with a patterning cascade model of development. *Journal of Anatomy* **217(3)**:245–253 DOI 10.1111/j.1469-7580.2010.01265.x.

**Skinner MM, Leakey MG, Leakey LN, Manthi FK, Spoor F. 2020.** Hominin dental remains from the Pliocene localities at Lomekwi, Kenya (1982–2009). *Journal of Human Evolution* **145**:102820 DOI 10.1016/j.jhevol.2020.102820.

**Skinner MM, Wood BA, Boesch C, Olejniczak AJ, Rosas A, Smith TM, Hublin JJ. 2008.** Dental trait expression at the enamel-dentine junction of lower molars in extant and fossil hominoids. *Journal of Human Evolution* **54(2)**:173–186 DOI 10.1016/j.jhevol.2007.09.012.

**Smith TM, Houssaye A, Kullmer O, Le Cabec A, Olejniczak AJ, Schrenk F, De Vos J, Tafforeau P. 2018.** Disentangling isolated dental remains of Asian Pleistocene hominins and pongines. *PLOS ONE* **13(11)**:e0204737 DOI 10.1371/journal.pone.0204737.

**Smith TM, Reid DJ, Dean MC, Olejniczak AJ, Martin LB. 2007.** Molar development in common chimpanzees (*Pan troglodytes*). *Journal of Human Evolution* **52(2)**:201–216 DOI 10.1016/j.jhevol.2006.09.004.

**Suwa G. 1990.** A comparative analysis of hominid dental remains from the Sungura and Usno formations. Ph.D. Dissertation, University of California, Berkeley.

**Suwa G, White TD, Howell FC. 1996.** Mandibular postcanine dentition from the Shungura Formation, Ethiopia: crown morphology, taxonomic allocations, and Plio-Pleistocene hominid evolution. *American Journal of Physical Anthropology* **101**:247–282 DOI 10.1002/(SICI)1096-8644(199610)101:2<247::AID-AJPA9>3.0.CO;2-Z.

**Suwa G, Wood BA, White TD. 1994.** Further analysis of mandibular molar crown and cusp areas in Pliocene and early Pleistocene hominids. *American Journal of Physical Anthropology* **93(4)**:407–426 DOI 10.1002/ajpa.1330930402.

**Tobias PV. 1991.** *The skulls, endocasts, and teeth of Homo habilis: pt. 1–4.* Cambridge: Cambridge University Press.

**Turner CG, Nichol CR, Scott GR. 1991.** Scoring procedures for key morphological traits of the permanent dentition: the Arizona State University dental anthropology system. In: Kelley MA, Larsen CS, eds. *Advances in Dental Anthropology.* New York: Wiley-Liss, 13–32.

**Villmoare B, Kimbel WH, Seyoum C, Campisano CJ, Di Maggio EN, Rowan J, Braun DR, Arrowsmith JR, Reed KE. 2015.** Early *Homo* at 2.8 Ma from Ledi-Geraru, Afar, Ethiopia. *Science* **347(6228)**:1352–1355 DOI 10.1126/science.aaa1343.

**Visualization Sciences Group. 2010.** AVIZO, Version 6.3. Visualization Sciences Group, Bordeaux.

**Weidenreich F. 1937.** *The dentition of sinanthropus pekinensis: a comparative odontography of the Hominids.* Beijing: Geological Survey of China.

**Wollny G, Kellman P, Ledesma-Carbayo MJ, Skinner MM, Hublin JJ, Hierl T. 2013.** MIA-A free and open source software for gray scale medical image analysis. *Source Code for Biology and Medicine* **8(1)**:20 DOI 10.1186/1751-0473-8-20.

**Wood BA. 1991.** *Koobi Fora research project: volume 4—Hominid cranial remains.* Oxford: Clarendon Press.

**Wood BA, Abbott SA. 1983.** Analysis of the dental morphology of Plio-pleistocene hominids—I. Mandibular molars: crown area measurements and morphological traits. *Journal of Anatomy* **136**:197–219.

**Xing S, Martinón-Torres M, De Castro JMB. 2018.** The fossil teeth of the Peking Man. *Scientific Reports* **8(1)**:1–11 DOI 10.1038/s41598-018-20432-y.

**Zanolli C, Kullmer O, Kelley J, Bacon A-M, Demeter F, Dumoncel J, Fiorenza L, Grine FE, Hublin J-J, Nguyen AT. 2019.** Evidence for increased hominid diversity in the Early to Middle Pleistocene of Indonesia. *Nature Ecology & Evolution* **3(5)**:755–764 DOI 10.1038/s41559-019-0860-z.

**Zanolli C, Mazurier A. 2013.** Endostructural characterization of the *H. heidelbergensis* dental remains from the early Middle Pleistocene site of Tighenif, Algeria. *Comptes Rendus Palevol* **12(5)**:293–304 DOI 10.1016/j.crpv.2013.06.004.

**Zanolli C, Schillinger B, Kullmer O, Schrenk F, Kelley J, Rössner GE, Macchiarelli R. 2020.** When X-rays do not work. characterizing the internal structure of fossil hominid dentognathic remains using high-resolution neutron microtomographic imaging. *Frontiers in Ecology and Evolution* **8**:42 DOI 10.3389/fevo.2020.00042.